



ELSEVIER

Thermochimica Acta 255 (1995) 281–295

thermochimica
acta

Synthesis, spectral and structural characterization and thermal decomposition kinetics of dinitrato (*N,N,N',N'*-tetra-*n*-butyl aliphatic diamide)uranyl(II) by thermogravimetric analysis

Zhenrong Lu ^{a,*}, Jianping Sun ^a, Li Yang ^a, Hanzhang Wang ^b,
Zhengbai Cao ^b

^a *The Central Laboratory, Suzhou University, Suzhou, Jiangsu 215006, People's Republic of China*

^b *Department of Chemistry, Suzhou University, Suzhou, Jiangsu 215006, People's Republic of China*

Received 28 July 1993; accepted 2 October 1994

Abstract

Uranyl complexes of the type $[\text{UO}_2(\text{TBAD})(\text{NO}_3)_2]$, where TBAD is *N,N,N',N'*-tetra-*n*-butyl aliphatic diamide, $\text{Bu}_2\text{NCO}(\text{CH}_2)_n\text{CONBu}_2$, with *n* being 1, 2, 3, 4, 6, 8 or 10, were all prepared (TBAD with *n* = 0 failed to form a complex of this type) and characterized by elemental analysis, and UV–vis and IR spectroscopy. The complexes were found to have a chelate structure with three bidentate ligands, one TBAD molecule and two NO_3^- groups, all coordinated through O atoms. Using single-crystal XRD, the complex with *n* = 2 in TBAD was revealed to have a deformed hexagonal bipyramid structure with a large organic ligand chelate ring. The thermal decomposition studies of the complexes were carried out in nitrogen atmosphere using TG–DTG techniques. The kinetic parameters (non-isothermal method) for the main TBAD decomposition step were evaluated using the method suggested by Málek, Šesták, Koga et al. Based on the above characterizations the effects of carbon chain length in TBAD on the structure, stability, and thermal behaviour of the complexes, were carefully observed and discussed. The results showed that not only the *E* value, but also the TBAD decomposition pattern and mechanism for the complex with *n* = 1 in TBAD are distinct from those of all the others.

Keywords: Chelate; Kinetics; Ligand; TBAD; Uranyl

* Corresponding author.

1. Introduction

Tetramethyl-substituted malonamide and adipamide are known extraction agents which complex mainly rare-earth metal ions such as La, Ce, Pr and Nd [1]. In addition, disubstituted aliphaticamides have also been reported to be extracting agents in the industrial application of solvent extraction, which is mainly used as an alternative to tri-*n*-butyl phosphate (TBP) in both the selective separation of uranium(VI) from thorium and the recovery of uranium and plutonium from highly irradiated nuclear fuels [2]. So far, however, there has been little information concerning the preparation of isolated complexes of these with uranyl or thorium. Moreover, knowledge of the effect of the structure of the ligand on the stability, structure and thermal behaviour of the complexes is still inadequate, but such knowledge would contribute to a better selection of the proper extracting agent, to the investigation of the extracting mechanism for uranium, and to the study of the structural chemistry of uranium.

In this paper, the preparation of a series of *N,N,N',N'*-tetra-*n*-butyl aliphatic diamides (TBAD), $\text{Bu}_2\text{NCO}(\text{CH}_2)_n\text{CONBu}_2$ (where *n* is 0, 1, 2, 3, 4, 6, 8 or 10), and of the cited complexes of type $[\text{UO}_2\text{L}(\text{NO}_3)_2]$ (where L is TBAD with *n* = 1, 2, 3, 4, 6, 8 or 10) is described. Their stereochemistry and molecular structure have been obtained from spectral and single-crystal XRD studies. The non-isothermal decomposition kinetics of the complexes under a dynamic nitrogen atmosphere has been studied using the TG–DTG technique. The kinetic parameters and the mechanism for their main TBAD decomposition steps have also been evaluated and studied employing the method suggested by J. Málek, J. Šesták, N. Koga and coworkers [3–7]. Based on the above characterizations of the complexes, the effect of the carbon chain length of TBAD on the structure and properties of $[\text{UO}_2(\text{TBAD})(\text{NO}_3)_2]$ is described.

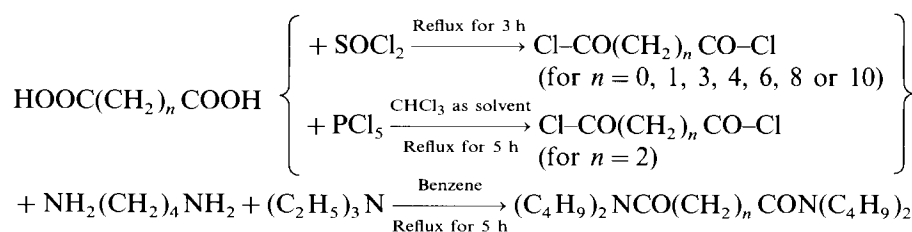
2. Experimental

2.1. Materials

All the reagents used were Analar grade and were used without further purification.

2.2. Synthesis

One of the starting materials for the synthesis of the ligand $\text{Bu}_2\text{NCO}(\text{CH}_2)_n\text{CONBu}_2$ (TBAD) is diacyl chloride, $\text{ClOC}(\text{CH}_2)_n\text{COCl}$, which was prepared by reaction of the appropriate dicarboxylic acid, $\text{HOOC}(\text{CH}_2)_n\text{COOH}$, with either SOCl_2 (for the preparation of diacyl chloride with *n* = 0, 1, 3, 4, 6, 8 or 10) or PCl_5 (for diacyl chloride with *n* = 2). By reference to the procedure given in the literature

Scheme 1. Synthesis of *N,N,N',N'*-tetra-*n*-butyl aliphatic diamide (TBAD).

[8], the ligand TBAD can then be obtained from the reaction of 1,4-diaminobutane, triethylamine and the above-described appropriate diacyl chloride (2.1 : 2 : 1 molar ratio) in benzene solution, with vigorous stirring in an ice–salt bath and with the reaction temperature held below 5°C.

Scheme 1 summarizes the synthesis of the ligands described in this paper.

To synthesize the complex $\text{UO}_2(\text{TBAD})(\text{NO}_3)_2$, TBAD was dissolved in warm petroleum ether (at 60–90°C), and 10 ml of the resulting solution was mixed with 10 ml of a solution of $\text{UO}_2(\text{NO}_3)_2 \cdot 6\text{H}_2\text{O}$ in 3 N nitrate acid (1 : 1 equimolar ratio) in an iodine number flask. The mixture was shaken well. A pale yellow precipitate appeared, and was then filtered off, and washed with deionized water and petroleum ether. This product was recrystallized from toluene, washed with petroleum ether again, and dried in vacuum for elemental analysis.

It is interesting to note that the reaction of $\text{UO}_2(\text{NO}_3)_2$ with TBAD with $n = 0$, i.e. $\text{Bu}_2\text{NCO-CONBu}_2$, failed to yield a product.

2.3. Apparatus

Microanalyses of carbon, nitrogen and hydrogen were performed on a Carlo-Erba model 1106 elemental analyser. The UV–visible spectra were recorded using a Shimadzu UV-240 UV–Visible spectrophotometer. Infrared spectra were taken in the region 4000–400 cm^{-1} on an Alpha Centauri FT-IR spectrometer, the solid compounds being mixed with fused potassium bromide and pressed into transparent discs. The crystalline and molecular structures were determined using an R3m/E single-crystal X-ray diffractometer.

Table 1
The kinetic models

Model	Symbol	$f(x)$
Šesták–Berggren equation	SB(m,n)	$x^m(1-x)^n$
Johnson–Mehl–Avrami equation	JMA(n)	$n(1-x)[- \ln(1-x)]^{1-1/n}$
Reaction order equation	RO(n)	$(1-x)^n$
Two-dimensional diffusion	D2	$1/[- \ln(1-x)]$
Jander equation	D3	$3(1-x)^{2/3}/2[1-(1-x)^{2/3}]$
Ginstling–Brounshtein equation	D4	$1.5[(1-x)^{-1/3}-1]$

Table 2

Analytical data (calculated values in parentheses) and comparison of the characteristic IR absorption $\nu(\text{co})$ between complexes and ligands

No.	Complex ^a	Analytical data			$\nu(\text{co})/\text{cm}^{-1}$		$\Delta\nu(\text{co})/\text{cm}^{-1}$
		C/%	H/%	N/%	Ligand	Complex	
1	$n = 1$	31.78 (31.67)	5.44 (5.27)	7.74 (7.78)	1641.5	1624.2 1579.5	17.3 62.0
2	$n = 2$	32.38 (32.70)	5.45 (5.45)	7.45 (7.63)	1641.5	1584.2 1579.8	57.3 61.7
3	$n = 3$	33.45 (33.69)	5.63 (5.65)	7.42 (7.48)	1641.5	1579.8	61.7
4	$n = 4$	34.32 (34.65)	5.85 (5.81)	7.11 (7.35)	1641.5	1577.9	63.7
5	$n = 6$	36.70 (36.46)	6.26 (6.12)	7.02 (7.09)	1641.5	1572.1	69.4
6	$n = 8$	38.25 (38.14)	6.45 (6.33)	6.73 (6.85)	1643.5	1572.1	71.4
7	$n = 10$	40.10 (39.72)	6.72 (6.62)	6.41 (6.62)	1643.5	1572.0	71.5

^a Complex $\text{UO}_2[\text{Bu}_2\text{NCO}(\text{CH}_2)_n\text{CONBu}_2](\text{NO}_3)_2$ with $n = 1, 2, 3, 4, 6, 8$ or 10 .

Thermogravimetric and thermal decomposition kinetics studies of all the complexes were performed on a Delta series TGA-7 thermogravimetric analyser in pure nitrogen flowing at a rate of 20 ml min^{-1} . The samples were heated at $2.5, 5.0, 10.0$ or $15.0^\circ\text{C min}^{-1}$ from 35 to 740°C , with approximately the same sample weight ($3\text{--}4 \text{ mg}$), to minimize heat transfer and mass transfer limitation [9].

3. Theory

Kinetic investigations of solid-state reactions have shown that the processes involved are generally complex [10,11], and that both the activation energy E and pre-exponential factor A are mutually correlated, which probably leads to an unreliable result [12]. Recently, a new complete method was therefore proposed by Málek, Šesták, Koga and coworkers [3–7], allowing reliable kinetic analysis and interpretation of non-isothermal TA data. As the method has been thoroughly described in the cited literatures, here we give only a brief outline, referring the reader to the original papers for further details.

The general kinetic equation in non-isothermal studies is

$$\frac{dx}{dT} = \frac{A}{\beta} \exp(-E/RT)f(x) \quad (1)$$

where x is the reaction fraction at the temperature T , A the pre-exponential factor, β the constant heating rate, E the activation energy, R the gas constant, T the temperature and $f(x)$ a function depending on the actual reaction mechanism. The most frequently used $f(x)$ functions [13] are summarized in Table 1.

3.1. Calculation of the activation energy E

Because of the strong mutual interdependence of the parameters E and A in Eq. (1), it has been suggested that the so-called multiple-scan methods available [14–16] be applied for calculation of the activation energy from several sets of kinetic data taken at various heating rates. In the present study, the Kissinger method was used to obtain E values. In addition, the Friedman method was also used to check the invariance of E with respect to α , which is one of the basic assumptions in kinetic analysis.

3.2. Determination of the kinetic model

Two special functions $Y(\alpha)$ and $Z(\alpha)$ which can easily be obtained by simple transformation of the experimental data are defined and a combination of the shape of function $Y(\alpha)$ with both the parameters α_M and α_P^∞ , at which the functions $Y(\alpha)$ and $Z(\alpha)$ have a maximum respectively, allows the determination of the most suitable kinetic models.

3.3. Calculation of the kinetic exponents n (or m)

To calculate the kinetic exponents, the appropriate equations depending on the kinetic model determined in the above step can be employed.

3.4. Calculation of the pre-exponential factor

Knowing the value of the activation energy and the kinetic model, the pre-exponential factor can be calculated.

4. Results and discussion

4.1. Elemental analysis and solubility

The complexes prepared, listed in Table 2, are barely soluble in water, slightly soluble in toluene, and readily soluble in dichloroethane, acetone, alcohol, etc. The analytical results agree with the proposed formulae, namely $\text{UO}_2\text{L}(\text{NO}_3)_2$.

4.2. UV-visible spectra

Two strong absorptions at 41 045 and 24 096 cm^{-1} were observed in the spectrum of free UO_2^{2+} ($\text{UO}_2(\text{NO}_3)_2$ in aqueous solution). In the case of the complex ($[\text{UO}_2\text{L}(\text{NO}_3)_2]$ in ethanol solution), these absorptions shift to 40 323 and 23 697 cm^{-1} respectively. This shift to lower frequencies has been suggested as being due to the coordination of the organic ligand to the metal ion.

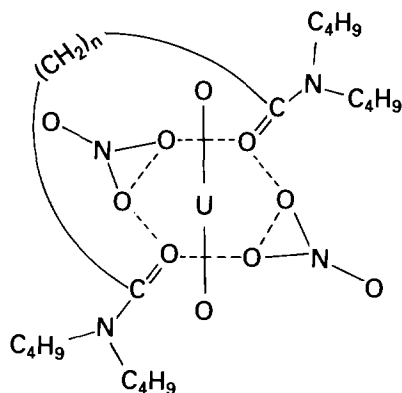


Fig. 1. Assumed molecular structure of the complexes.

4.3. Infrared spectra

In their IR spectra, the complexes showed a strong adsorption at 934 cm^{-1} arising from an asymmetric stretching vibration of UO_2^{2+} [17], and absorptions at $747, 808, 1031, 1264, 1497$ and 1571 cm^{-1} assigned to the vibrations of coordinated NO_3^- [18,19]. A shift to lower frequency for $\nu(\text{C}=\text{O})$ near 1642 cm^{-1} was found, indicating coordination of the carbonyl group, which is listed in Table 2.

As seen from Table 2, and $\Delta\nu(\text{co})$ increases with increasing length of carbon chain in TBAD. There is only one $\nu(\text{co})$, arising from a stretching vibration of $\text{C}=\text{O}$, for complexes 3–7, which, together with the results of the elemental analysis of the complexes and the knowledge of the normal coordination number of UO_2^{2+} , suggests that both carbonyl groups of each TBAD molecule are equally coordinated to UO_2^{2+} through O atoms, and that the molecular structure of the titled

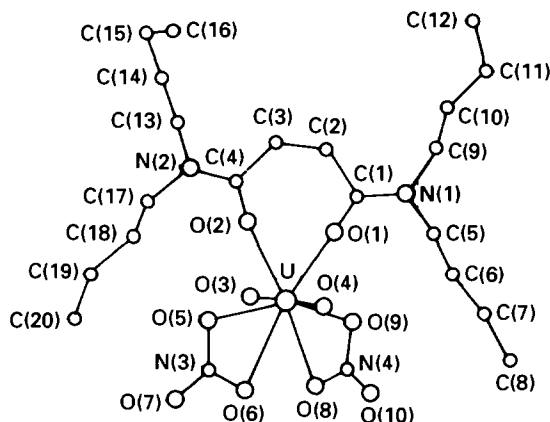


Fig. 2. Molecular structure of complex $\text{UO}_2[\text{Bu}_2\text{NCO}(\text{CH}_2)_2\text{CONBu}_2](\text{NO}_3)_2$ (together with the numbering scheme).

Table 3

Thermal decomposition data for complexes studied in dynamic nitrogen atmosphere from TG and DTG analyses (measured at $\beta = 5^\circ\text{C min}^{-1}$)

No.	Complex ^a	Temperature			Loss of mass/wt%		Probable composition of expelled group	
		$T_i/^\circ\text{C}$	$T_f/^\circ\text{C}$	$T_m/^\circ\text{C}$	TG	Theory ^b		
1	$n = 1$	I	212	365	294	45.10	45.30	TBAD
		II	365	677	620	15.79	15.73	$2\text{NO}_2 + (2/3)\text{O}_2$
2	$n = 2$	I	214	292	275	60.89 ^c	61.03 ^c	$3\text{C}_4\text{H}_9$
		II	292	340	305	23.84	23.33	TBAD ^d
		III	340	673	355	22.53	23.01	$2\text{NO}_2 + (2/3)\text{O}_2$
3	$n = 3$	I	210	296	278	15.57	15.44	$3\text{C}_4\text{H}_9$
		II	296	358	313	61.94 ^c	61.78 ^c	TBAD ^d
		III	358	744	367	22.59	22.86	$2\text{NO}_2 + (2/3)\text{O}_2$
4	$n = 4$	I	231	284	273	24.72	24.49	$2\text{C}_4\text{H}_9$
		II	284	337	322	62.24 ^c	62.49 ^c	TBAD ^d
		III	337	715	368	14.98	14.86	$2\text{NO}_2 + (2/3)\text{O}_2$
5	$n = 6$	I	236	292	282	63.78 ^c	63.18 ^c	$2\text{C}_4\text{H}_9$
		II	292	343	332	14.18	14.43	TBAD ^d
		III	343	613	369	35.41	35.72	$2\text{NO}_2 + (2/3)\text{O}_2$
6	$n = 8$	I	220	290	273	14.83	14.34	$2\text{C}_4\text{H}_9$
		II	290	356	336	64.42 ^c	64.49 ^c	TBAD ^d
		III	356	625	368	14.14	13.96	$2\text{NO}_2 + (2/3)\text{O}_2$
7	$n = 10$	I	223	306	291	65.92 ^c	65.70 ^c	C_4H_9
		II	306	387	372	6.58	6.75	TBAD ^d
		III	387	667	612	45.70	46.70	$2\text{NO}_2 + (2/3)\text{O}_2$
					14.52	13.39		
					66.80 ^c	66.84 ^c		

^a Complex $\text{UO}_2[\text{Bu}_2\text{NCO}(\text{CH}_2)_n\text{CONBu}_2](\text{NO}_3)_2$ with $n = 1, 2, 3, 4, 6, 8$ or 10 . ^b The value was calculated on the basis of the possible decomposition reaction equation (see text). ^c Total loss of mass in wt%. ^d The remainder of ligand after the first step. ^e For complexes 2, 4, 5 and 6, stage III actually consists of two consecutive and partly overlapping steps.

complexes may then be supposed to be formed as in Fig. 1, that is, a large chelate ring consisting of a carbon chain, $-(\text{CH}_2)_n-$, two carbonyl groups $-\text{C}=\text{O}-$, and a uranium ion U.

Of particular interest is the split in the absorption peak $\nu(\text{CO})$ for complexes 1 and 2, which may be caused by some difference in the coordination extent between the two carbonyl groups, owing to the steric hindrance of the shorter carbon chain in TBAD 1 and 2. This assumption has already been supported by further study by X-ray diffraction, which reveals that the bond lengths of the two C=O groups in complex 2 are a little different, 1.229 and 1.262 Å, respectively. The same argument may explain the fact that, in this study, $\text{Bu}_2\text{NCO}-\text{CONBu}_2$, with the shortest

carbon chain, does not even react with $\text{UO}_2(\text{NO}_3)_2$ to form an isolated solid complex.

4.4. Single-crystal X-ray diffractometry

Many attempts at growing crystals of the title complexes in a range of different solvents have failed to yield a single crystal suitable for crystallographic study. So far, only a crystal of complex 2, $\text{UO}_2(\text{Bu}_2\text{NCO}(\text{CH}_2)_2\text{CON}-\text{Bu}_2(\text{NO}_3)_2$ which was grown from CH_2Cl_2 has been obtained. Its structure was established by single-crystal X-ray diffractometry, and is shown in Fig. 2. The crystal is quadratic, space group $I41/a$, with $a = b = 33.207(8)$, $c = 10.711(4)$ Å, $\alpha = \beta = \gamma = 90.00(0)^\circ$. The molecular structure reveals that one organic ligand molecule and two nitrate groups in complex 2 are all bidentate ligands [20]: each of them attaches directly to the uranium ion through its two oxygen atoms, together with the other two of UO_2^{2+} itself. The uranium ion is surrounded by a total of eight oxygen atoms, forming a distorted hexagonal bipyramid which probably results from the steric repulsive interaction between the large chelate ring of the organic ligand and the two small ones of nitrate groups. It is obvious that the result here is consistent with the structure predicted by spectral analysis.

Detailed results from the crystallographic study will be reported elsewhere.

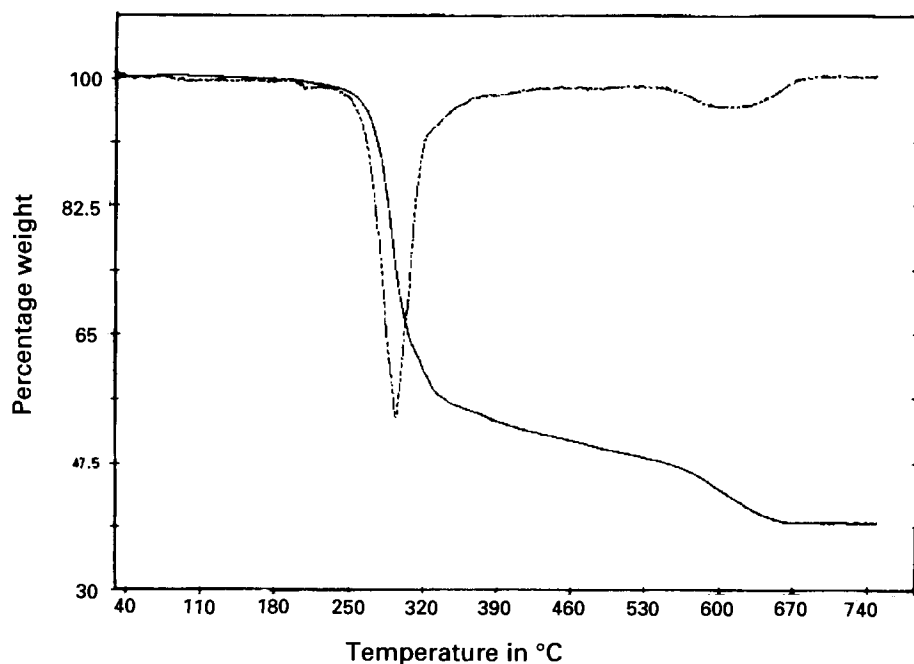


Fig. 3. TG and DTG trace for $\text{UO}_2[\text{Bu}_2\text{NCOCH}_2\text{CONBu}_2](\text{NO}_3)_2$ ($\beta = 5^\circ\text{C min}^{-1}$).

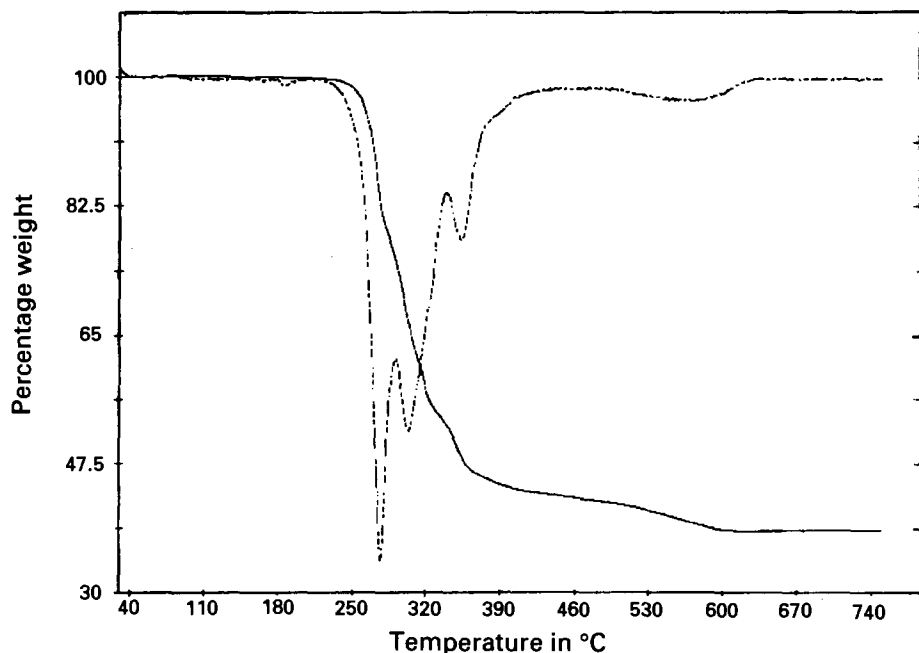


Fig. 4. TG and DTG trace for $\text{UO}_2[\text{Bu}_2\text{NCO}(\text{CH}_2)_2\text{CONBu}_2](\text{NO}_3)_2$ ($\beta = 5^\circ\text{C min}^{-1}$).

4.5. Thermal behaviour

All the complexes studied have a fairly wide stability range and essentially the same pattern of thermal decomposition, except complex 1. The temperature range and DTG peaks, together with the percentage of mass loss measured at $\beta = 5^\circ\text{C min}^{-1}$ and probable composition of expelled groups, are presented in Table 3. Some representative TG–DTG curves are shown in Figs. 3, 4 and 5.

The DTG curve for complex 1 shows two peaks. The first step in the decomposition of this complex corresponds to the removal of a TBAD molecule, followed by the step of releasing NO_2 and O_2 .

It is quite interesting to note that, in the case of all the other complexes, the TDG curves reveal three or even four decomposition stages. The mass loss for these complexes suggests that the initial weight loss which is complete at about 290°C is due to the elimination of some butyl groups from the TBAD molecule. The IR spectra of the intermediate compounds after this stage show the presence of the coordinated C=O bond, and its elemental analysis also supports our assumption. From the point of view of bond strength [21], it seems reasonable for a possible break to occur at the Bu–N bond because the C–N bond has almost the lowest bond energy ($303.6 \text{ kJ mol}^{-1}$) of all the concerned bonds in the TBAD molecule, namely C–H ($411.0 \text{ kJ mol}^{-1}$), C–C ($345.6 \text{ kJ mol}^{-1}$) and C=O ($798.9 \text{ kJ mol}^{-1}$). The phenomenon that some butyl groups break before the loss of the whole TBAD molecule also suggests that the Bu–N bond is weaker than the coordinated O–U

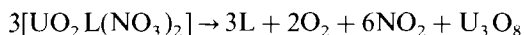
bond for complexes 2–7. In contrast with this, the unique way in which complex 1 decomposes once again demonstrates the relative weakness of the O–U coordination bond in complex 1, as described above.

The second stage of decomposition for complexes 2–7 corresponds to the removal of the remainder of the TBAD, followed by the loss of NO_2 and O_2 , which starts at about 350°C and seems to have either a single-step decomposition mode (for complexes 3 and 7) or two consecutive and partly overlapping steps (for complexes 2, 4, 5 and 6).

The peak temperature of the TBAD (or its residue) decomposition step appears to increase slightly with increasing carbon chain length in TBAD (Fig. 6).

The residue weight for all the complexes studied after the final decomposition is in good agreement with the theoretical value required for U_3O_8 , which is consistent with the result described in our previous work [19] and in the literature [22,23].

Thus, the possible decomposition reaction for the studied complexes may be [19]



4.6. Thermal decomposition kinetics

Kinetic studies have only been made on the step corresponding to the loss of TBAD (or its remainder) which is the only clear-cut step with a well-resolved peak in the DTG curve and is also the most meaningful step in this study.

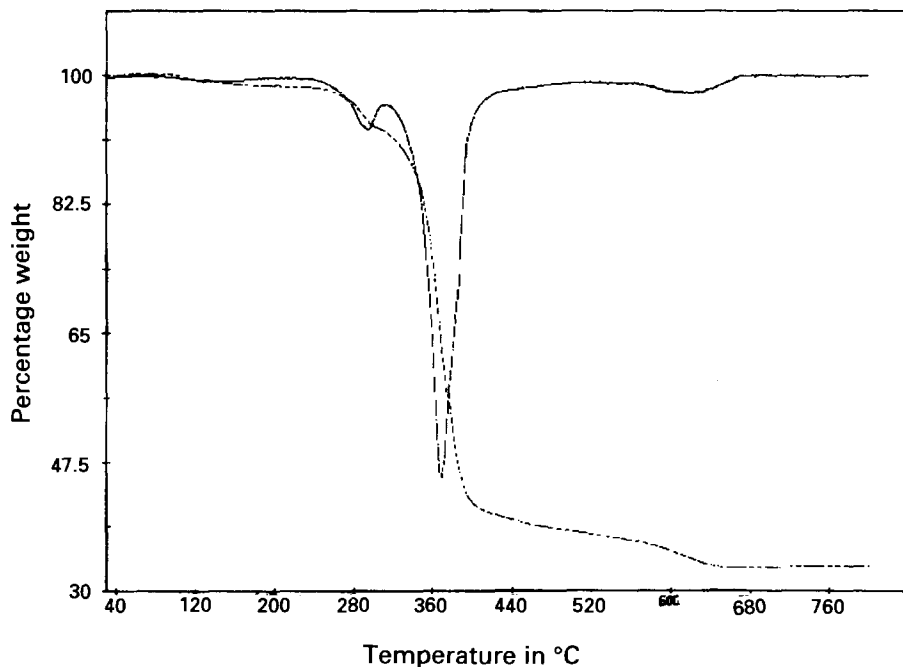


Fig. 5. TG and DTG trace for $\text{UO}_2[\text{Bu}_2\text{NCO}(\text{CH}_2)_{10}\text{CONBu}_2](\text{NO}_3)_2$ ($\beta = 5^\circ\text{C min}^{-1}$).

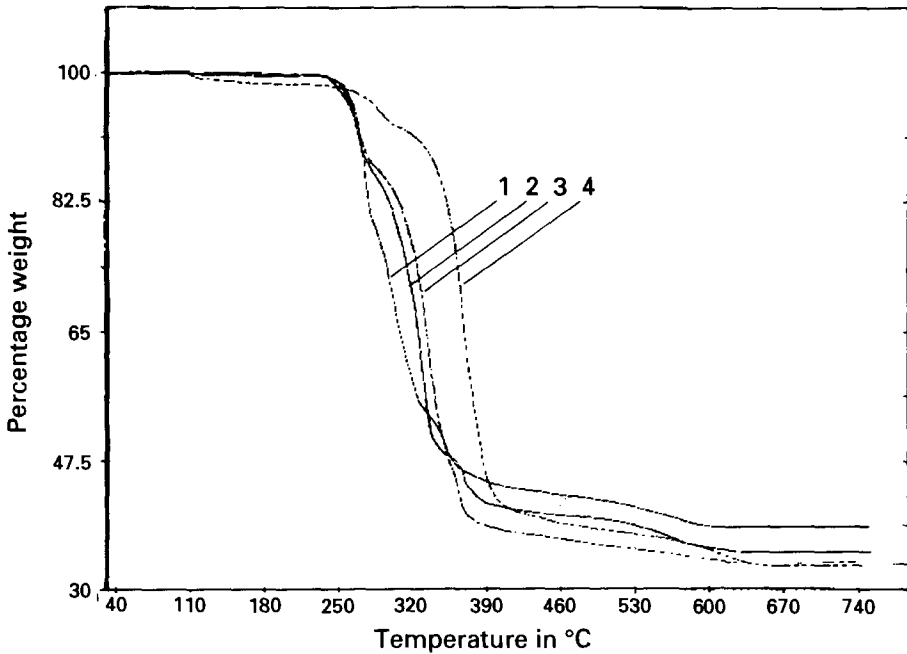


Fig. 6. TG curves for complexes $\text{UO}_2[\text{Bu}_2\text{NCO}(\text{CH}_2)_n \text{CONBu}_2](\text{NO}_3)_2$: curve 1, $n = 2$; curve 2, $n = 6$; curve 3, $n = 8$; curve 4, $n = 10$ ($\beta = 5^\circ\text{C min}^{-1}$).

The activation energy values for all the complexes determined by the Kissinger and Friedman methods are listed in Table 4. It can be seen that the values of activation energy obtained by the two methods are in reasonable agreement, and that E values calculated using the Friedman method for any complex are generally independent of the value of α , which has provided a check for the constancy of E during the course of reaction; therefore the E values obtained using the Kissinger

Table 4

The values of E (in kJ mol^{-1}) calculated by the Kissinger and Friedman methods

No.	Complexes ^a	Kissinger	Friedman					Av. ^b
			$\alpha = 0.10$	0.25	0.50	0.75	0.90	
1	$n = 1$	152	147	148	143	148	144	146
2	$n = 2$	172	171	166	167	169	170	169
3	$n = 3$	175	180	182	175	177	176	178
4	$n = 4$	170	168	166	163	169	165	166
5	$n = 6$	193	190	181	180	190	184	185
6	$n = 8$	186	193	192	188	189	186	190
7	$n = 10$	182	178	180	177	184	177	179

^a Complex $\text{UO}_2[\text{Bu}_2\text{NCO}(\text{CH}_2)_n \text{CONBu}_2](\text{NO}_3)_2$ with $n = 1, 2, 3, 4, 6, 8$ or 10 . ^b The average value of E by the Friedman method at various α values.

Table 5
The characteristic features of the functions $Y(\alpha)$ and $Z(\alpha)$

No.	Complex ^a	Shape of $Y(\alpha)$	α_M	α_P^∞
1	$n = 1$	Concave	0.009	0.593
2	$n = 2$	Convex	0.202	0.514
3	$n = 3$	Convex	0.422	0.436
4	$n = 4$	Convex	0.273	0.668
5	$n = 6$	Convex	0.338	0.826
6	$n = 8$	Convex	0.280	0.663
7	$n = 10$	Convex	0.175	0.792

^a Complex $\text{UO}_2[\text{Bu}_2\text{NCO}(\text{CH}_2)_n\text{CONBu}_2](\text{NO}_3)_2$ with $n = 1, 2, 3, 4, 6, 8$ or 10 .

equation were used for the next calculations. The important feature and parameter values thus obtained, such as α_M and α_P^∞ , corresponding to the maxima of both the $Y(\alpha)$ and $Z(\alpha)$ curves are summarized for all the studied complexes in Table 5.

It is evident that the values of these parameters conform to the RO(n) model for complex 1 and the SB(m, n) model for all the other complexes respectively. The kinetic parameters calculated for these models are presented in Table 6. In addition, Figs. 7 and 8 show some typical $Y(\alpha)$ and $Z(\alpha)$ dependences.

As a chelate ligand, the average values of the activation energy E of the TBAD decomposition step are as high as 180 kJ mol^{-1} , except in the case of complex 1. Taking into account the possible experimental error and the fact that the TBAD decomposition patterns for these complexes are not exactly the same, it does not seem possible for us to determine a regularity in the variation of the E value with the molecular structure of the ligand.

However, it is interesting to note that, not only the E value, but also the TBAD decomposition pattern and mechanism for complex 1 are distinctive from those of all the other complexes.

Table 6
Kinetic parameters and mechanism

No.	Complex ^a	$E/(\text{kJ mol}^{-1})$	$\ln(A/s^{-1})$	KM ^b	m	n
1	$n = 1$	152	30.68	RO	–	1.15
2	$n = 2$	172	38.72	SB	0.374	1.483
3	$n = 3$	175	35.78	SB	0.968	1.326
4	$n = 4$	170	33.28	SB	0.280	0.747
5	$n = 6$	193	20.00	SB	0.127	0.248
6	$n = 8$	186	35.73	SB	0.293	0.754
7	$n = 10$	182	32.98	SB	0.083	0.393

^a Complex $\text{UO}_2[\text{Bu}_2\text{NCO}(\text{CH}_2)_n\text{CONBu}_2](\text{NO}_3)_2$ with $n = 1, 2, 3, 4, 6, 8$ or 10 . ^b Kinetic model.

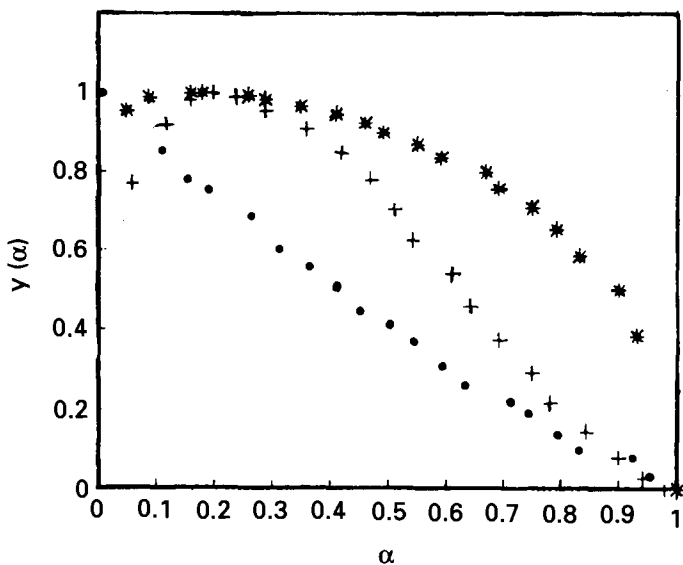


Fig. 7. Normalized $Y(\alpha)$ functions corresponding to the TBAD decomposition kinetic data measured at a heating rate of $5^{\circ}\text{C min}^{-1}$ for complexes $\text{UO}_2[\text{Bu}_2\text{NCO}(\text{CH}_2)_n\text{CONBu}_2](\text{NO}_3)_2$: \cdot , complex 1 with $n=1$; +, complex 2 with $n=2$; *, complex 7 with $n=10$.

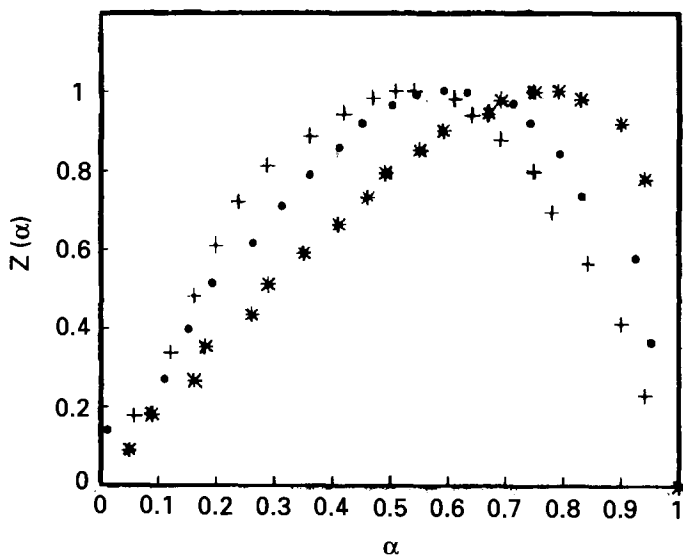


Fig. 8. Normalized $Z(\alpha)$ functions corresponding to the TBAD decomposition kinetic data measured at a heating rate of $5^{\circ}\text{C min}^{-1}$ for complexes $\text{UO}_2[\text{Bu}_2\text{NCO}(\text{CH}_2)_n\text{CONBu}_2](\text{NO}_3)_2$: \cdot , complex 1 with $n=1$; +, complex 2 with $n=2$; *, complex 7 with $n=10$.

5. Conclusions

N,N,N',N'-tetra-*n*-butyl aliphatic diamide (TBAD), $\text{Bu}_2\text{NCO}(\text{CH}_2)_n\text{CONBu}_2$ can react with uranyl nitrate to form an isolated complex only on condition that the carbon chain in TBAD is long enough, i.e. *n* must be greater than unity. The complex formed has a chelate structure with all the ligands, namely one TBAD molecule and two nitrate groups, as bidentate ligands. These complexes are stable up to about 210°C, and their decompositions are complete at a temperature within the range 610–750°C.

The variation in the carbon chain length in organic ligand molecules exerts more or less influence on the structure of the complex, the equality in coordination ability of both carbonyl bonds in TBAD, the thermal decomposition pattern and the peak temperatures of corresponding steps in the DTG curve for TBAD, but has no significant effect on the decomposition kinetic parameters and mechanism of the complexes studied (except complex 1) in the present work.

Acknowledgements

The authors express their gratitude to Dr N. Koga of Hiroshima University, Japan for providing his papers which were very helpful in the kinetic analysis of this work and to Mr X. Hu for writing part of the computer program used in this study.

References

- [1] G.X. Xu and C.Y. Yuan, Solvent Extraction for Rare-Earth Metal. Science Press, Beijing, 1987, p. 41, in Chinese.
- [2] G.M. Gasparini and G. Grossi, Solvent Extraction and Ion Exchange, 4(6) (1986) 1233.
- [3] J. Málek, Thermochim. Acta, 138 (1989) 109.
- [4] J. Málek and V. Smrcka, Thermochim. Acta, 186 (1991) 153.
- [5] J. Málek, Thermochim. Acta, 200 (1992) 257.
- [6] N. Koga, J. Málek, J. Šesták and H. Tanaka, Netsu Sokutei, 20(4) (1993) 210.
- [7] J. Šesták and J. Málek, Solid State Ionics, 63–65 (1993) 245.
- [8] S.R. Sandler and W. Karo, Organic Functional Group Preparations, Academic Press, New York and London, 1968, p. 278.
- [9] F. Carrasco, Thermochim. Acta, 213 (1993) 115.
- [10] W.E. Brown, D. Dallimore and A.K. Galwey, in C.H. Bamford and C.F.H. Tipper (Eds.), Comprehensive Chemical Kinetics, Vol. 22, Elsevier, Amsterdam, 1980.
- [11] J. Šesták, V. Šatáva and W. Wendlandt, Thermochim. Acta, 7 (1973) 333.
- [12] N. Koga and J. Šesták, Thermochim. Acta, 182 (1991) 201–208.
- [13] J. Šesták, Thermophysical Properties of Solids, Their Measurement and Theoretical Analysis, Elsevier, Amsterdam, 1984.
- [14] H.E. Kissinger, Anal. Chem., 29 (1957) 1702.
- [15] T. Ozawa, J. Therm. Anal., 2 (1979) 301.
- [16] H.L. Friedman, J. Polym. Sci., Part C, 6 (1964) 183.
- [17] C. Panattoni, R. Graziani, B.Z. Bangoli and G. Bombieri, Inorg. Chem., 8 (1969) 320.

- [18] J.G. Allpress and A.N. Hambly, *Aust. J. Chem.*, 12 (1959) 569.
- [19] L. Yang, Z.R. Lu, Z.B. Cao and H.Z. Wang, *Thermochim. Acta*, 210 (1992) 205.
- [20] K.F. Purcell and J.C. Kotz, *Inorganic Chemistry*, W.B. Saunders Company, Philadelphia, 1977, p. 518.
- [21] J.E. Huheey, *Inorganic Chemistry*, 3rd edn., Harper International Edition, Cambridge, 1983, p. A-32.
- [22] G.X. Xu, W.Q. Wang, G.X. Wu, H.C. Gao and N. Shi, *Principle of Extraction Chemistry*, Shanghai Science and Technology Publishing House, 1984, in Chinese.
- [23] F.A. Cotton and G. Wilkinson, *Advanced Inorganic Chemistry*, 4th edn., Wiley, New York, 1980.